Chemical Engineering Journal 161 (2010) 346–354

Contents lists available at ScienceDirect

Chemical Engineering Journal

journal homepage: www.elsevier.com/locate/cej

Monoglyceride synthesis by glycerolysis of methyl oleate on solid acid–base catalysts

Cristián A. Ferretti, Agostina Soldano, Carlos R. Apesteguía, J. Isabel Di Cosimo*

Catalysis Science and Engineering Research Group (GICIC)- INCAPE (UNL-CONICET) Santiago del Estero 2654, (3000) Santa Fe, Argentina

ARTICLE INFO

Article history:
Received 3 June 2009
Received in revised form 17 July 2009
Accepted 21 July 2009

Keywords:
Glycerol
Monoglyceride
Fatty acid methyl ester
Base catalysis
Glycerolysis

ABSTRACT

The synthesis of monoglycerides by glycerolysis of methyl oleate, an unsaturated fatty acid methyl ester, was studied on acid–base solid catalysts as an alternative to the current commercial technology that uses liquid base catalysts. Initially, the reaction conditions such as catalyst particle size and stirring rate required for operating the four-phase semi-continuous reactor under a kinetically controlled-regime were determined. Then the optimization of the reaction parameters for achieving high monoglyceride yields was performed using MgO. MgO compared favorably with the corresponding homogeneously catalyzed process. In fact, when using high reaction temperatures (493–523 K), glycerol/methyl oleate molar ratios between 2 and 6, and catalyst/reactant ratios of about 30 g/mol, glycerolysis of methyl oleate yields up to 77% monoglycerides in 2 h, a much higher value than those usually obtained via the liquid base-catalyzed homogeneous process (40–60%).

The acid–base site requirements for the glycerolysis reaction were investigated using single oxides with different electronegativities. A good correlation was found between the catalytic activity and the base site density. In addition, results show that glycerolysis of methyl oleate requires strong base sites such as those of MgO.

1. Introduction

Due to the increasing prices of fossil fuels the biomass-derived fuel industry is growing worldwide. In particular, biodiesel production capacity of Europe, USA, Brazil and Argentina currently totals about 28 million tons per year.

During biodiesel synthesis by oil or fat transesterification, glycerol (Gly) is obtained as the main co-product (Scheme 1), representing 10% of the biodiesel production. Therefore, the increasing production of biodiesel around the world generates a Gly surplus that is becoming a matter of economic and environmental concern since the drop of the Gly price has forced the producers to burn or sell Gly without even refine it. Thus, new applications intended to convert glycerol into value-added chemicals are highly desirable not only to improve the economics of biodiesel production but also for ecological reasons.

Due to its structure and properties Gly participates in the formulation or synthesis of many compounds such as food products, cosmetics, pharmaceuticals, liquid detergents and antifreeze [1]. Gly can also be used in the synthesis of hydrogen [2], liquid fuels [3], fuel additives [4] and chemicals [1,5]. Among the latter, monoglyceride (MG) synthesis by Gly esterification or transesterification, is an attractive option to transform this biomass-derived compound into fine chemicals.

Monoglycerides, the glycerol monoesters of fatty acids, are molecules consisting of a hydrophilic head and a hydrophobic tail having surfactant and emulsifying properties that help hydrophilic and lipophilic substances mix together. Therefore, they can be used in food, detergent, plasticizer, cosmetic and pharmaceutical formulations [5,6].

MGs can be synthesized from glycerol using triglycerides (TG), fatty acids (FA) or fatty acid methyl esters (FAME). However, the process from FAME, Scheme 2, presents several advantages, e.g., FAME is less corrosive than FA, has lower hydrophobic character than TG and exhibits higher miscibility with glycerol; therefore, the process can be carried out at lower temperatures (393–503 K) than TG transesterification (≈533 K) [6]. The reaction route from FAME allows the production of MGs with a definite acyl group composition (FAMEs are easier to separate by fractional distillation than FAs) whereas in TG glycerolysis the products contain the acyl group distribution of the oil or fat [7].

Enzymatic and liquid acid- or liquid base-catalyzed production of MG has been extensively investigated lately [1,6,7]. However, enzymatic processes are difficult to set up and expensive and not very efficient because of enzyme reusability issues. On the other hand, the two main liquid-catalyzed synthesis routes to produce MG from glycerol involve strong mineral acids such as sulfuric and phosphoric acids or strong bases such as $Ca(OH)_2$ and KOH; both

* Corresponding author. Tel.: +54 342 4555279; fax: +54 342 4531068.
E-mail address: dicosimo@fiq.unl.edu.ar (J.I. Di Cosimo).

1385-8947/$ – see front matter © 2009 Elsevier B.V. All rights reserved.
doi:10.1016/j.cej.2009.07.041

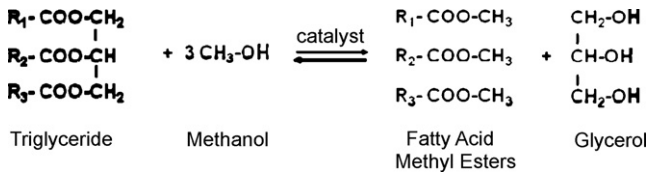

Scheme 1. Biodiesel synthesis from triglycerides.

processes entail concerns related to high toxicity, corrosion, and disposal of spent acid or base materials. In addition, in the homogeneously catalyzed processes, the reaction products contain only 40–60% MG, the rest being DG and TG. Several purification steps are required to obtain food or pharmaceutical grade MG, such as neutralization of the reaction media and discoloration followed by expensive molecular distillation [5,6].

The use of solid catalysts for MG synthesis, presents not only the known environmental and practical advantages but also provides the opportunity to increase the MG yield by developing a catalyst with tunable structural, surface acid–base and textural properties specifically designed to promote the reaction.

In spite of the technological benefits of using solid catalysts and of the MG synthesis from FAME, industrial implementation of a heterogeneously catalyzed process using solid base catalysts able to replace the current technology using liquid bases with similar performance is still a challenge.

In this paper we study the Gly transesterification with an unsaturated FAME, oleic acid (C18:1) methyl ester, under heterogeneously catalyzed conditions using solid catalysts with different acid–base properties. Our goals were to implement this reaction under kinetically controlled-conditions and to optimize the reaction parameters for maximum MG yield. Therefore, the effect of the stirring rate and catalyst particle size was investigated in order to rule out diffusional limitations. Moreover, the effect of reaction temperature, catalyst load and Gly/FAME ratio on the MG yield was also studied. In addition, the chemical nature and the acid–base requirements of the active site for promoting the MG synthesis were also investigated.

2. Materials and methods

2.1. Catalyst synthesis

Magnesium oxide was prepared by hydration with distilled water of low-surface area commercial MgO (Carlo Erba 99%; 27 m^2/g). Then the resulting $Mg(OH)_2$ was decomposed and stabilized in a N_2 flow for 1 h at 373 K, then for 1 h at 623 K, and finally for 18 h at 773 K to obtain high-surface area MgO [8]. The catalyst was ground, sieved and separated in three different lots before decomposition in N_2. The resulting average particle size lots were: <100 μm; 100–177 μm; 177–250 μm.

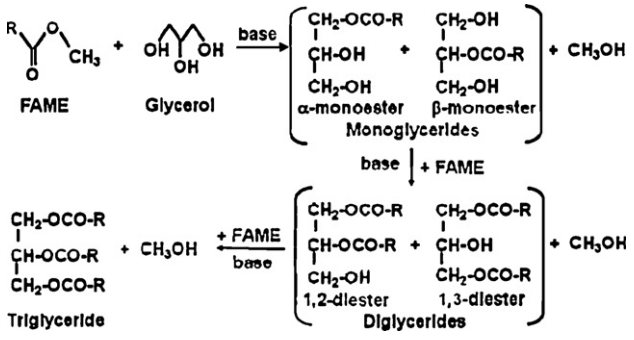

Scheme 2. Monoglyceride (MG) synthesis via transesterification (glycerolysis) of FAME with Gly and consecutive reactions to diglycerides (DG) and triglycerides (TG).

Y_2O_3, ZnO and CeO_2 precursors were prepared by precipitation method at a constant pH of 10. An aqueous solution of the metal cation nitrate was contacted with a basic solution of K_2CO_3 and KOH by dropwise addition of both solutions into a stirred beaker containing 350 cm^3 of distilled deionized water held at 333 K. The precipitates formed were aged in their mother liquor for 2 h at 333 K and then filtered, washed with boiling distilled water until K^+ was no longer detected in the filtrate, and dried at 348 K overnight. The ZrO_2 precursor, i.e., $Zr(OH)_4$ was obtained by precipitation of zirconium oxychloride with ammonium hydroxide. All these precursors were decomposed in N_2 or air at 723–773 K overnight in order to obtain the corresponding oxides. Nb_2O_5 was prepared by decomposition at 773 K of commercial hydrated niobium pentoxide HY340 from Companhia Brasileira de Metalurgia e Mineracao (CBMM). Alumina was a commercial sample of γ-Al_2O_3 Cyanamid Ketjen CK 300.

2.2. Catalyst characterization

BET surface areas were determined by N_2 physisorption at 77 K in a NOVA-1000 Quantachrom sorptometer.

Catalyst base site densities (n_b) were measured by temperature-programmed desorption (TPD) of CO_2 preadsorbed at room temperature. Samples were pretreated in situ in a N_2 flow at 723–773 K, cooled down to room temperature, and then exposed to a flowing mixture of 3% of CO_2 in N_2 until surface saturation was achieved (5 min). Weakly adsorbed CO_2 was removed by flushing with N_2. Finally, the temperature was increased to 773 K at a ramp rate of 10 K/min. The flow containing the desorbed CO_2 was passed through a methanation reactor and converted in CH_4 on a Ni/Kieselghur catalyst at 673 K; CH_4 was then continuously analyzed using a flame ionization detector (FID). Efficiency of the CO_2 conversion in CH_4 was checked periodically by introducing known amounts of CO_2 and CH_4 in the methanation reactor.

Acid site densities were determined by using TPD of NH_3. Samples (150 mg) were treated in He (~100 cm^3/min) at 723–773 K for 0.5 h and exposed to a 1.01% NH_3/He stream at room temperature until surface saturation. Weakly adsorbed NH_3 was removed by flowing He at 60 cm^3/min for 0.5 h. Temperature was then increased to 773 K at 10 K/min, and the NH_3 concentration in the effluent was measured by mass spectrometry (MS).

The chemical nature of adsorbed surface CO_2 species was determined by Infrared Spectroscopy (IR) after CO_2 adsorption at room temperature and sequential evacuation at increasing temperatures. The sample was pressed in a wafer and degassed in vacuum at 723–773 K for 1 h and then cooled down to room temperature. The spectrum of the pre-treated catalyst was then taken. After admission of 5 kPa of CO_2 and evacuation at 298, 373, 473 and 573 K, the CO_2 adsorption spectra were recorded at room temperature. Spectra of the adsorbed species were obtained by subtracting the catalyst spectrum. Data were collected in a Shimadzu FTIR Prestige-21 spectrometer using an inverted T-shaped cell fitted with CaF_2 windows containing the sample pellet. The absorbance scale was normalized to 20 mg.

2.3. Catalytic tests

The transesterification of methyl oleate (Fluka, >60.0%, with 86% total C18 + C16 esters as determined by gas chromatography), with glycerol (Aldrich, 99.0%,) was carried out at 473–523 K in a seven-necked cylindrical glass reactor with mechanical stirring equipped with a condenser to remove the methanol generated during reaction. In the text FAME and Gly stand for methyl oleate and glycerol, respectively.

Gly/FAME molar ratios in the range of 1–6 and a catalyst/FAME ratio (W_{cat}/n^0_{FAME}) of 9–30 g/mol were used. The reactor was oper-

ated in a semi-batch regime at atmospheric pressure under flowing N_2 (35 cm^3/min). First, the liquid reactants were introduced and the reactor was flushed with nitrogen, then the reactor was heated to reaction temperature under stirring (400–700 RPM). Catalyst was pretreated ex situ at 773 K for 6 h to remove adsorbed water and carbon dioxide and kept overnight at 373 K in flowing N_2 until used, then quickly transferred to the reactor without exposing it to air to start the reaction. The reactor was assumed to be perfectly mixed.

For the homogeneously catalyzed experiment, a 25 wt.% sodium methoxide (NaMeO) solution was prepared by reacting NaOH with methanol under stirring [9].

2.4. Sample analysis and quantification

Reaction products: α- and β-glyceryl monooloeates (MGs), 1,2- and 1,3-glyceryl dioleates (diglycerides, DGs) and glyceryl trioleate (triglyceride, TG) were analyzed by gas chromatography (GC) after silylation to improve compound detectability [10]. Quantification was carried out using authentic standards of glyceryl trioleate (Sigma, 65.0%) and a commercial mixture of glyceryl mono and dioleate of known composition (Fluka, 71.5% MG and 25.3% DG).

Twelve samples of the reaction mixture were extracted and analyzed during the 8-h catalytic run. Reaction samples were centrifuged at room temperature at 3000 RPM to separate the glycerol-containing phase from the FAME-rich phase; both phases were analyzed following the same procedure, for instance, 10 μL of "fatty phase" (FAME-rich phase) were measured, weighted and placed in test tubes. Known amounts of pyridine solution of n-hexadecane (Sigma, >99.0%) and cholesterol (Aldrich, 95.0%) were added as internal standards of the silylation reaction. Then, the reaction products were converted to trimethylsilylether derivatives with N,O-bis (trimethylsilyl) acetamide (BSA, Fluka, >95%) and trimethylchlorosilane (TMCS, Fluka, >98%). Hexane solutions of the resulting mixtures were then analyzed by GC in a SRI 8610C gas chromatograph equipped with a flame ionization detector (FID), on-column injector port and a HP-1 Agilent Technologies 15 m × 0.32 mm × 0.1 μm capillary column.

Conversion (X_{FAME}, referred to the total content of esters in the reactant), selectivity (S) and yield (Y) were calculated through the following equations (n_j, mol of product j; MG = monoglycerides (both isomers), DG = diglycerides (both isomers), TG = triglyceride):

$$X_{FAME}\,(\%)\frac{n_{MG}+2n_{DG}+3n_{TG}}{n_{MG}+2n_{DG}+3n_{TG}+n_{FAME}}\times 100$$

$$S_{MG}\,(\%)\frac{n_{MG}}{n_{MG}+2n_{DG}+3n_{TG}}\times 100$$

$$S_{DG}\,(\%)\frac{2n_{DG}}{n_{MG}+2n_{DG}+3n_{TG}}\times 100$$

$$S_{TG}\,(\%)\frac{3n_{TG}}{n_{MG}+2n_{DG}+3n_{TG}}\times 100$$

$$Y_j\,(\%) = X_{FAME}S_j \times 100$$

3. Results and discussion

3.1. Reaction parameter optimization using MgO

Previous to the heterogeneously catalyzed glycerolysis and for comparison purposes, a homogeneously catalyzed reaction was performed using sodium methoxide (NaMeO) as a catalyst in a ratio of $W_{NaMeO}/n^0_{FAME} = 5.5$ g/mol at 408 K with a Gly/FAME = 2 (molar ratio) and a stirring rate of 550 RPM [11,12]. After 5 h, a FAME conversion of ≈100% was achieved with a maximum MG yield of 59%, a DG yield of 24% and a TG yield of 17%.

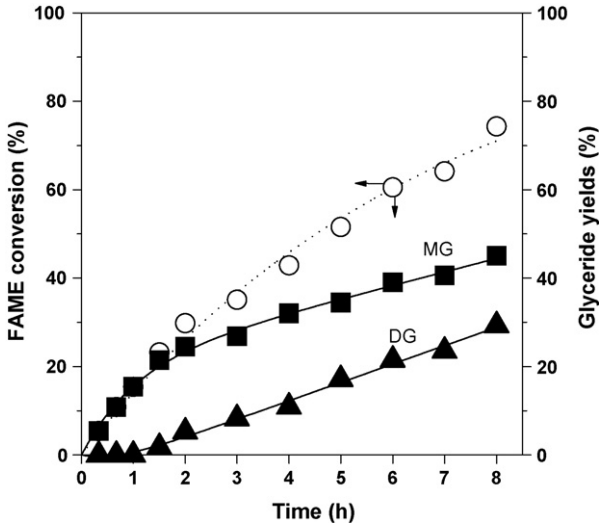

Fig. 1. FAME conversion and glyceride yields [MgO, Gly/FAME = 2; T = 493 K; $W_{cat}/n^0_{FAME} = 11$ g/mol FAME].

Then, two MgO-promoted preliminary tests were carried at 493 K by loading the reactor first with pure glycerol and then with pure methyl oleate. No conversion was detected in any of these experiments.

A typical heterogeneously catalyzed methyl oleate glycerolysis on MgO ($W_{cat}/n^0_{FAME} = 11$ g/mol FAME) at 493 K and Gly/FAME = 2, is shown in Fig. 1. Results show that monoglycerides can be obtained with reasonable yields (45%) in 8 h using MgO. Initially, only MG formation was observed. Then, as the reaction proceeded, a second transesterification took place forming diglycerides (DG) from MG and FAME (Scheme 2). At the end of the run the DG yield was 29%. No TG formation was observed in these catalytic tests using MgO in contrast with those performed with NaMeO.

In both, the homogeneously and the heterogeneously catalyzed experiments the main MG isomer was α-glyceryl monooleate (Scheme 2) resulting from participation of the two primary OH groups of Gly in the glycerolysis reaction. Similarly, 1,3-glyceryl dioleate was the main DG isomer.

The heterogeneously promoted reaction system for monoglyceride synthesis is outlined in Scheme 3. The reactor consists of four

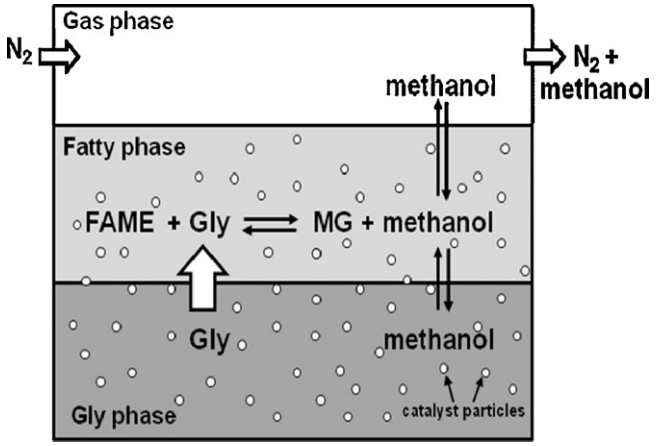

Scheme 3. Four-phase reactor for the heterogeneously catalyzed monoglyceride synthesis.

phases: the solid catalyst; the bottom liquid layer formed by the Gly phase; the liquid "fatty phase" containing FAME and glyceride products and the gas phase containing N_2 and methanol.

FAME is not soluble in Gly and Gly is barely soluble in the fatty phase. Thus, the reaction occurs in the fatty phase where both reactants may coexist; for the reaction to occur, Gly has to be transferred from the more hydrophilic glycerol phase to the more hydrophobic fatty phase where it is immediately consumed. Therefore, Gly is not detected in that phase at short reaction times but as FAME conversion increases and glycerides are formed, the Gly concentration in the fatty phase increases because of the glycerides surfactant properties that enhance Gly solubility in the hydrophobic phase. On the other hand, glycerides were never found in the glycerol phase under our heterogeneous catalysis conditions. The byproduct methanol forms in the fatty phase but is more soluble in the glycerol phase. However, under the reaction conditions used here, methanol was released to the gas phase and hardly detected in any of the liquid phases.

Initially we investigated the operative conditions required to rule out diffusional limitations in this four-phase reaction system. Only mass-transfer limitations were investigated since transesterification reactions are known to have low reaction enthalpies [13,14].

In the reaction system of Scheme 3 several mass interfacial gradients can occur such as those at the liquid–liquid (Gly phase-fatty phase interface) and liquid–solid (mass-transfer resistance around the catalyst particles in the fatty phase) boundaries as well as those inside the catalyst pores.

Mass gradients at the liquid–liquid interface are strongly dependent on the stirring rate. Thus, if the overall reaction rate were controlled by the reactant diffusion rate through this interface, then FAME conversion would increase by increasing the stirring rate. To investigate the presence of liquid–liquid interfacial gradients, the effect of the stirring rate on the reaction kinetics was studied. Several 3-h catalytic tests were carried out on MgO using stirring rates in the range of 400–700 RPM, without changing any other operational parameter. FAME conversion was not significantly changed by increasing the stirring rate from 400 to 700 RPM. Then, it was concluded that the reaction is not liquid–liquid diffusion-controlled under the present experimental conditions and we adopted the highest stirring rate (700 RPM) for performing the following experiments.

The reactant diffusion rates at the liquid–solid interface and inside the catalyst particles depend on the catalyst particle size. Thus, if the overall reaction rate were controlled by the reactant diffusion around or inside the catalyst particle, then FAME conversion would increase when decreasing the catalyst particle size. The effect of the MgO particle size on FAME conversion was investigated by carrying out several 3-h catalytic tests using three different particle size ranges (<100 μm; 100–177 μm and 177–250 μm), without changing any other reaction parameter. Only small differences within the experimental error were observed during the 3-h tests thereby confirming the absence of diffusional limitations inside or around the catalyst particles. However and for practical reasons to avoid flotation of small particles in the presence of the foam caused by the surfactant MG, we adopted the largest particle size range for the following catalytic experiments.

The stoichiometry of the MG reaction synthesis (Scheme 2) requires a glycerol to FAME (Gly/FAME) molar ratio of 1:1 but a glycerol excess is often used to drive the reaction forward and reach high FAME conversions. However, the effect of the glycerol excess on the kinetics of FAME glycerolysis over MgO is difficult to predict because glycerol is more hydrophilic than FAME and would be probably strongly adsorbed on the catalyst surface. In addition, Gly is more dense than FAME and has to be transferred to the fatty phase where the reaction occurs, even though it is little soluble in that phase. Therefore, the Gly/FAME ratio can affect the Gly solubility in the reaction zone.

In order to investigate the effect of Gly/FAME ratio on MG yield, 8-h catalytic tests were performed on MgO at 493 K with Gly/FAME molar ratios in the range of 1–6, using a constant catalyst/FAME ratio ($W_{cat}/n^0_{FAME} = 11$ g/mol) and variable molar amounts of Gly. Evolution of MG yield (Y_{MG}) curves, Fig. 2, indicates that at the beginning of the reaction there was no difference between the tests performed at increasing Gly/FAME ratios. However, at higher reaction times the catalytic tests carried out with Gly/FAME ratios above one produced significantly higher MG yields in comparison to that performed with stoichiometric reactant concentration (Gly/FAME = 1). In the latter, a maximum in the MG yield curve was observed because of the rapid consecutive DG formation. This MG yield maximum is not explained by a faster FAME transformation since the FAME conversion was about 40% at that point, but by the Gly consumption in the reaction zone. In fact, Gly conversion increased with decreasing the Gly/FAME ratio and for the stoichiometric reactant ratio the Gly transfer rate to the fatty phase was not rapid enough to maintain the FAME-Gly reaction going. Thus, MGs initially formed kept reacting with a second FAME molecule to form preferentially DGs that were the main reaction products at the end of the run (Scheme 2).

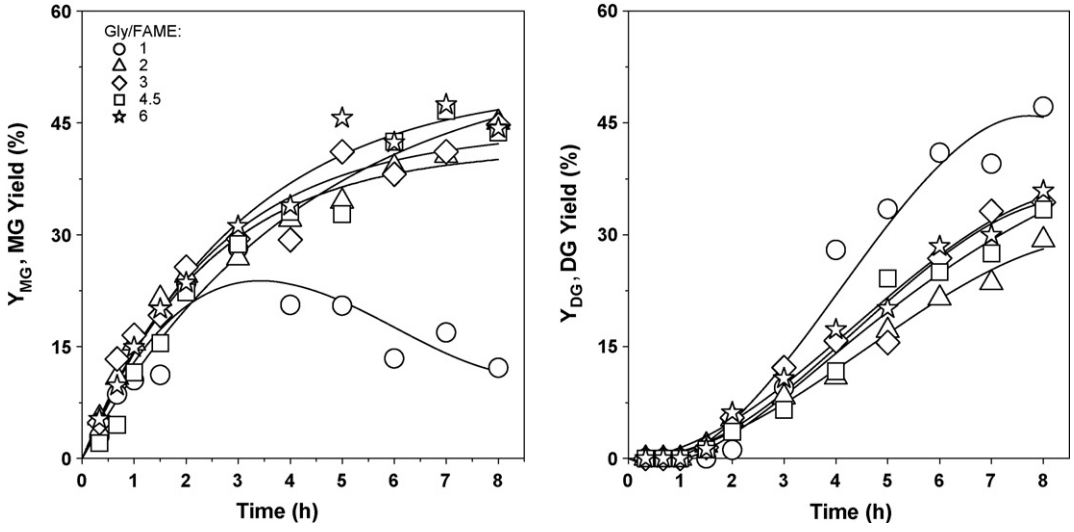

Fig. 2. Effect of the Gly/FAME ratio on MG and DG yields [T = 493 K; $W_{cat}/n^0_{FAME} = 11$ g/mol; particle size: 177–250 μm; stirring rate = 700 RPM; catalyst: MgO].

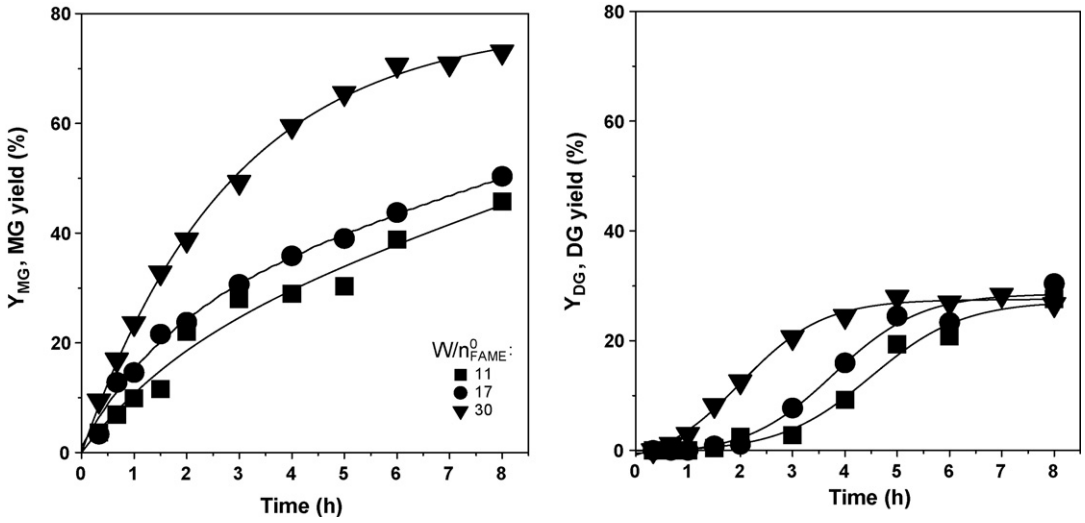

Fig. 3. Effect of the catalyst load on MG and DG yields [Gly/FAME = 4.5 (molar ratio); T = 493 K; Particle size: 177–250 μm; Stirring rate = 700 RPM; Catalyst: MgO].

Table 1
Physicochemical properties of different solid acid–base catalysts.

Catalyst	Electronegativity, χ_{oxide} (Pauling unit)	Surface area (m^2/g)	Base site density, n_b[a] (μmol/g)	Acid site density, n_a[b] (μmol/g)
MgO	2.12	192	655.0	15.0
Y_2O_3	2.27	54	280.0	12.0
CeO_2	2.37	75	147.0	21.0
ZnO	2.38	18	2.7	2.5
ZrO_2	2.51	83	58.0	22.0
Al_2O_3	2.54	230	14.0	101.0
Nb_2O_5	2.76	84	5.0	125.0

[a] By TPD of CO_2.
[b] By TPD of NH_3.

As a conclusion, Gly/FAME ratios higher than one have to be used in order to selectively obtain MGs. Gly/FAME ratios in the range of 2–6 gave similar results suggesting a zeroth reaction order with respect to Gly in the overall kinetics. Therefore, Gly/FAME ratios as low as 2 can be used without significantly affecting the MG yield.

The effect of the MgO catalyst load on the FAME conversion was also investigated. Several catalytic tests were conducted at 493 K with different catalyst/FAME ratios (W_{cat}/n^0_{FAME} = 11, 17 and 30 g/mol). In agreement with the absence of diffusional limitations, the FAME conversion was almost duplicated when the W_{cat}/n^0_{FAME} ratio was increased from 17 to 30 g/mol. On the other hand, product selectivity was independent of the catalyst load when compared at similar conversion levels. Therefore, the MG yield increased as the catalyst load increased, Fig. 3, as a consequence of the enhanced FAME conversion; a MG yield of 73% was attained in 8 h for the experiment with W_{cat}/n^0_{FAME} = 30 g/mol. This MG yield is much

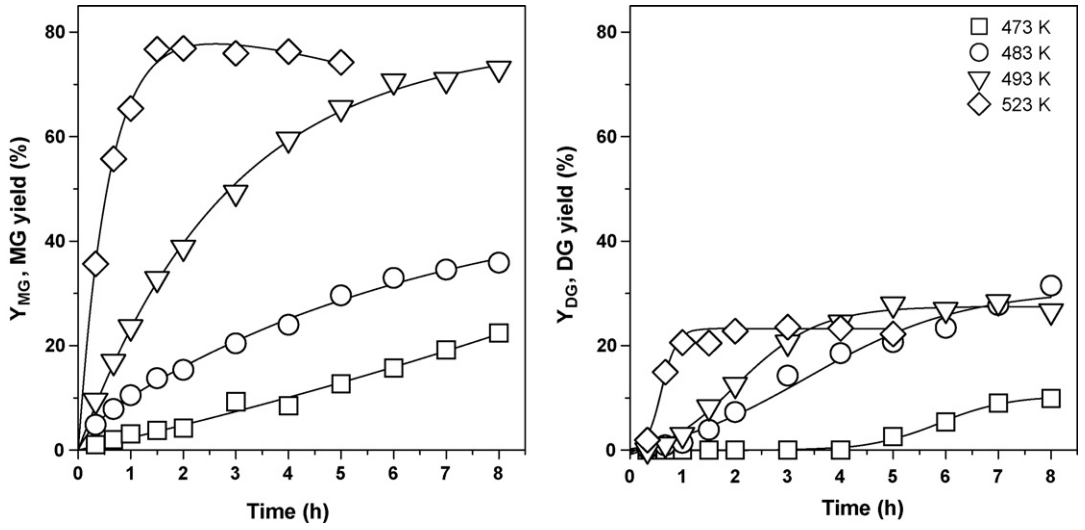

Fig. 4. Effect of the reaction temperature on MG and DG yields [Gly/FAME = 4.5 (molar ratio); W_{cat}/n^0_{FAME} = 30 g/mol; particle size: 177–250 μm; stirring rate = 700 RPM; catalyst: MgO].

higher than that measured at the end of our catalytic experiment using NaMeO (59%) and also than the typical MG yields obtained in commercial homogeneously catalyzed MG synthesis (40–60%) [5,6].

Variations of the reaction temperature modify not only the overall kinetic rate constant but also Gly solubility [14,15]. Therefore, an increase of the reaction temperature is expected to increase the FAME conversion. However, the increase of the reaction temperature is limited by undesirable product formation (polyglycerols on basic catalysts and acrolein on acidic catalysts) [16,17].

The effect of the reaction temperature on the catalyst activity and selectivity was investigated here by carrying out catalytic tests on MgO at 473, 483, 493 and 523 K using a Gly/FAME ratio of 4.5. As expected, FAME conversion significantly increased with the reaction temperature so that complete conversion was achieved in 2 h at 523 K in contrast to 4% at 473 K. The selectivity to MG improved at higher reaction temperatures at the expense of the DG selectivity when compared at similar FAME conversion levels. Thus, MG yield was significantly increased by increasing the reaction temperature as shown in Fig. 4. In summary, as a result of the combined effect of temperature on FAME conversion and MG selectivity, MG yields as high as 77% can be obtained at 523 K in just 2 h on MgO without thermal degradation of reactants or products and without formation of TG.

3.2. Monoglyceride synthesis on different acid–base oxides

3.2.1. Catalyst textural and acid–base properties

The BET surface area, electronegativity and acid and base site densities of the different oxides used in this work are reported in Table 1. Oxide electronegativities (χ_{oxide}) were calculated as the geometric mean of the atomic electronegativities using the Pauling's electronegativity scale. For an oxide with the formula M_nO_x, the bulk oxide electronegativity is [18]:

$$\chi_{oxide} = [(\chi_M)^n(\chi_O)^x]^{1/(n+x)}$$

The catalyst basic properties were determined by TPD of CO_2, Fig. 5. The base site density, n_b, was calculated by integration of TPD curves as the total amount of CO_2 desorbed from the catalysts, and the resulting values are reported in Table 1. In Fig. 6 the n_b values are plotted as a function of the electronegativity showing that they depended on the acid–base properties of the oxide metal cation so that the total base site density decreased with increasing oxide electronegativity. Thus, a n_b value of 655 μmol/g was quantified on MgO and whereas just 5 μmol/g were measured on Nb_2O_5.

The complex TPD profiles of Fig. 5 reveal the presence of surface base sites that bind CO_2 with different strength. Also, the TPD traces of Fig. 5 show that not only the n_b values are affected by the electronegativity of the oxide metal cation but also the binding energies of adsorbed CO_2 species. Whereas the most electronegative oxides of Table 1 were weakly or moderately basic (CO_2 desorption temperature at 350–400 K or ≈450 K), low-electronegativity oxides (MgO and Y_2O_3), presented an additional high-temperature desorption peak (≈550 K) arising from CO_2 adsorbed on stronger basic sites.

The catalyst acidic properties were determined by TPD of NH_3, Fig. 7. Acid site densities (n_a) calculated by integration of the NH_3 TPD profiles of Fig. 7 are reported in Table 1. As expected, the n_a values increased with increasing the catalyst electronegativity, Fig. 6. The strength of the catalyst acid sites also followed the electronegativity trend, as indicated in the NH_3 TPD curves by the high-temperature peak (≈580 K) found on the most electronegative solids such as Nb_2O_5, Al_2O_3 and ZrO_2. The other oxides presented essentially a single low-temperature desorption peak at about 400 K which revealed they are weakly or mildly acidic materials. The total NH_3 evolved from the stronger basic catalysts such as MgO and Y_2O_3 probably includes NH_3 adsorption and decomposition on acid–base pairs that gives rise to species such as M-NH_2^- (M = Mg^{2+} or Y^{3+}).

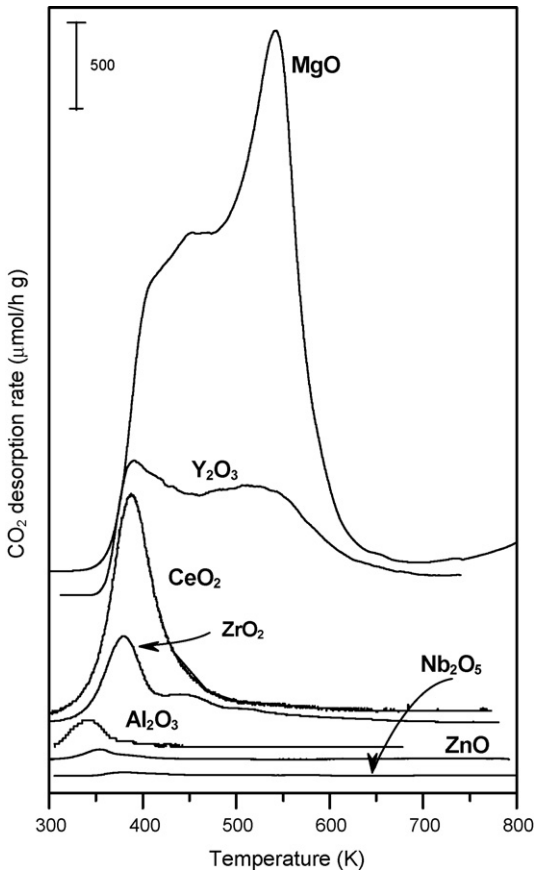

Fig. 5. TPD of CO_2 on different oxides.

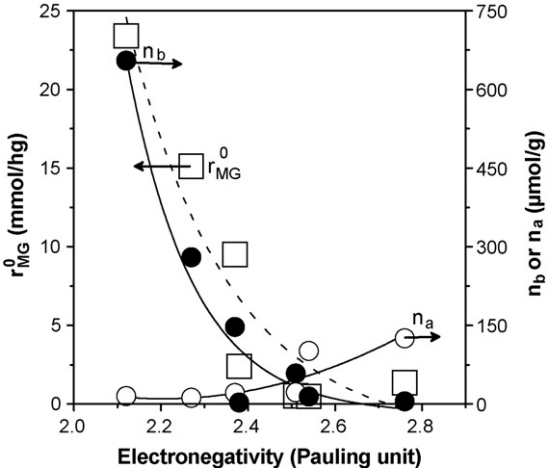

Fig. 6. Initial MG formation rate (r^0_{MG}) and total acid (n_a) and base (n_b) site densities as a function of oxide electronegativity [T = 493 K; Gly/FAME = 4.5 (molar ratio); W_{cat}/n^0_{FAME} = 30 g/mol; particle size: 177–250 μm; stirring rate = 700 RPM].

3.2.2. Effect of the catalyst acid–base properties on monoglyceride synthesis

The different single oxides of Table 1 were tested in the methyl oleate glycerolysis reaction. All the oxides produced exclusively monoglycerides and diglycerides during the 8-h experiments at 493 K. Fig. 8 presents the FAME conversions and glyceride yields

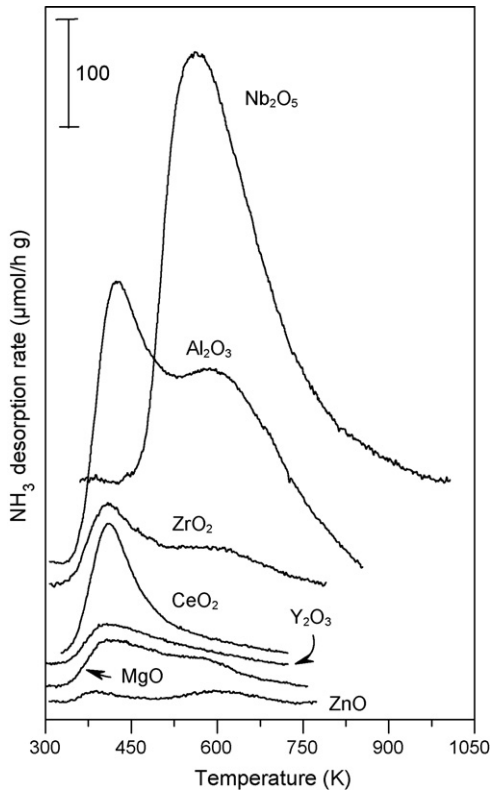

Fig. 7. TPD of NH_3 on different oxides.

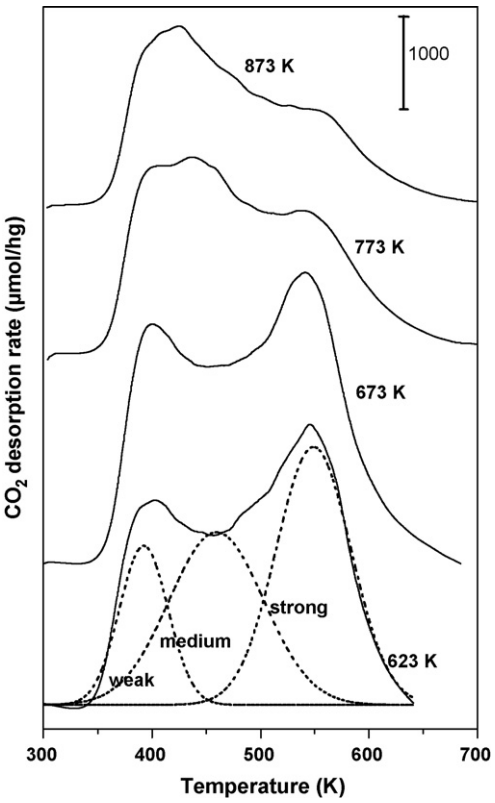

Fig. 9. TPD of CO_2 of MgO catalysts activated at different calcination temperatures.

as a function of reaction time where is clearly shown that basic oxides such as MgO, Y_2O_3 and CeO_2 converted more than 90% of FAME in less than 8 h. In contrast, acidic oxides such as Al_2O_3, ZrO_2 and Nb_2O_5 were less active for MG synthesis than basic oxides.

From the data of Fig. 8 we determined the initial MG formation rate (r^0_{MG}, mmol/gh) by calculating the initial slopes of the MG yield curves according to

$$r^0_{MG} = \frac{n^0_{FAME}}{W_{cat}} \left[\frac{dY_{MG}}{dt}\right]_{t=0},$$

where W_{cat} is the catalyst weight and n is the molar amount of FAME initially loaded in the reactor. The r^0_{MG} values were plotted as a function of the oxide electronegativity in Fig. 6 as well as those of n_b and n_a; a good correlation was found between the catalytic activity and the base site density what confirms that glycerolysis of methyl oleate is promoted on basic sites.

3.3. Identification of the active site

In order to get insight into the chemical nature of the basic site responsible for the glycerolysis activity, several additional experiments were carried out using a series of MgO catalysts treated at different calcination temperatures. The surface areas of MgO calcined at 623, 673, 773 and 873 K were 258, 183, 189 and 169 m^2/g, respectively.

Fig. 9 shows the TPD of CO_2 obtained for these MgO samples. Not only the total base site density (n_b) but also the strength distribution changed by increasing the calcination temperature as indicated by the different shapes of the TPD traces.

In Fig. 10, the MG initial formation rates (r^0_{MG}) as well as the n_b values are plotted as a function of the MgO calcination temperature. In agreement with the results of Fig. 6 obtained for several acid–base catalysts, a good correlation was observed between the initial activity and the base site density of the different MgO

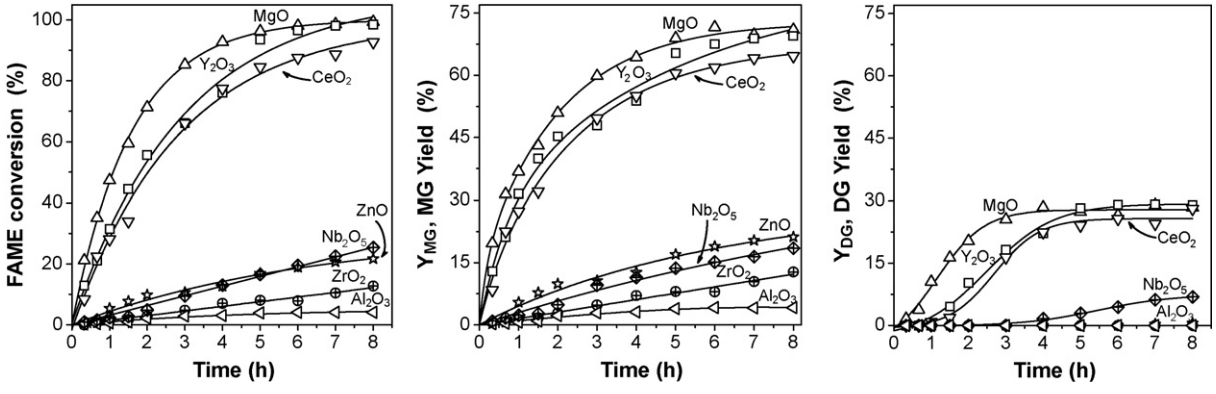

Fig. 8. FAME conversion and glyceride yields on different oxides. Reaction conditions as in Fig. 6.

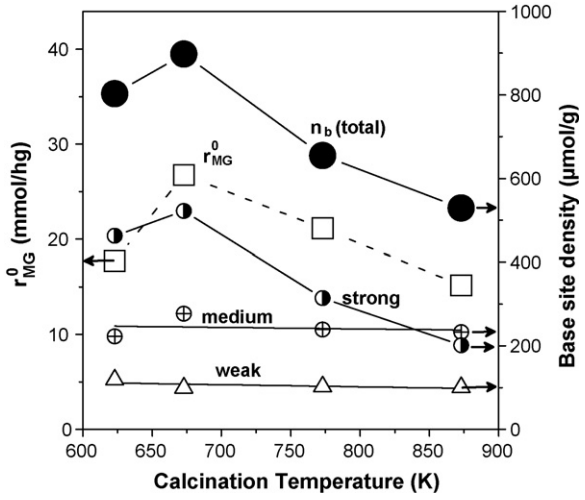

Fig. 10. Effect of the MgO calcination temperature on the initial MG formation rate (r^0_{MG}) and on the base site density distribution. Reaction conditions as in Fig. 6.

samples. The r^0_{MG} and n_b curves of Fig. 10 present both a maximum at 673 K.

The FTIR analysis of CO_2 adsorbed at room temperature and evacuated at 298, 373, 473 and 573 K was carried out on MgO treated at different calcination temperatures. Fig. 11 presents the CO_2 FTIR spectra obtained after CO_2 evacuation at 373 K. Overlapping broad infrared bands were observed in the 1700–1200 cm^{-1} region, confirming catalyst surface heterogeneity and formation of different carbonate species. In a previous work [19] we investigated the chemical nature of the adsorbed species on similar MgO and MgO-based catalysts by using FTIR of CO_2 and identified at least three different CO_2 adsorption species: unidentate carbonate, bidentate carbonate and bicarbonate. Unidentate carbonate formation requires isolated surface O^{2-} ions, i.e., low-coordination anions, such as those present in corners or edges and exhibits a symmetric O–C–O stretching at 1360–1400 cm^{-1} and an asymmetric O–C–O stretching at 1510–1560 cm^{-1}. Bidentate carbonate forms on Lewis acid–Brønsted base pairs (M–O pair site, M = metal cation) and shows a symmetric O–C–O stretching at 1320–1340 cm^{-1} and an asymmetric O–C–O stretching at 1610–1650 cm^{-1}. Bicarbonate species formation involves surface hydroxyl groups and shows a C–OH bending mode at 1220 cm^{-1} as well as symmetric and asymmetric O–C–O stretching bands at 1480 cm^{-1} and 1650 cm^{-1}, respectively [20,21].

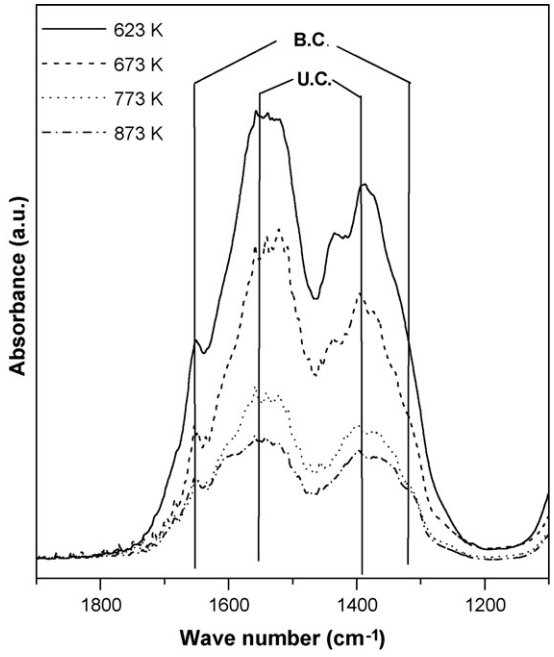

Fig. 11. FTIR spectra of CO_2 adsorbed species on MgO catalysts activated at different calcination temperatures [CO_2 adsorption at room temperature and evacuation at 373 K; B.C: bidentate carbonate; U.C: unidentate carbonate].

The bicarbonate species disappeared after evacuation at 373 K due to the weak basic nature of the surface OH^- groups of MgO. Contrarily, unidentate and bidentate carbonates remained on the surface even after evacuation at 573 K, but the unidentate species were more difficult to remove by evacuation at high temperatures. Thus, we determined the following base strength order for these surface oxygen species: low coordination O^{2-} anions > oxygen in Mg^{2+}–O^{2-} pairs > OH^- groups.

All the MgO catalysts of Fig. 11 exhibited unidentate and bidentate carbonate species but the higher band intensity of the unidentate carbonates suggests that the surface of the MgO catalysts contain mainly strongly basic low coordination oxygen anions. Clearly, as the calcination temperature increased the band intensity corresponding to CO_2 species retained on the strongest base sites (unidentate carbonate species) decreased more notoriously than that of the bidentate species. This result indicates surface smoothing after increasing the severity of the thermal treatment causing elimination of surface defects such as corners or edges where strongly basic oxygen anions are located.

Based on the identification of the surface oxygen species by IR, the contribution of weak (OH^- groups), medium (oxygen in Mg^{2+}–O^{2-} pairs) and strong (low coordination O^{2-} anions) base sites to the total base site density (n_b) was measured by deconvolution of the TPD curves of Fig. 9 using Gaussian functions. The deconvolution results were plotted in Fig. 10 as a function of the calcination temperature showing that the number of strong base sites presented a maximum at 673 K whereas the number of medium-strength and weak base sites remained almost constant. These results show that the catalytic performance of MgO treated at different calcination temperatures (r^0_{MG} values in Fig. 10) is essentially related to the change in the number of strong base sites.

In summary, it is inferred that the heterogeneously catalyzed monoglyceride synthesis on MgO is mainly promoted on strong base sites such as the low coordination oxygen anions.

4. Conclusions

The liquid-phase glyceryl monooleate (monoglyceride) synthesis by glycerolysis of methyl oleate is efficiently carried out on solid base catalysts such as MgO, Y_2O_3 and CeO_2. Therefore, solid bases offer an alternative technology to the current commercial processes that use environmentally unfriendly liquid bases.

The heterogeneously catalyzed monoglyceride synthesis is a four-phase reaction that may be conducted in kinetic control regime provided that appropriate operative conditions are used, namely: relatively high stirring rates (500–700 rpm) and mean catalyst particle sizes of up to 250 μm.

Monoglyceride yields of ≈73–77% are obtained on MgO using reaction temperatures in the range of 493–523 K and glycerol/methyl oleate ratios of 2 or higher. These monoglyceride yields are higher than those typically obtained via the homogeneously catalyzed process (40–60%). Diglycerides are the only byproducts formed by a consecutive transesterification step.

The glycerolysis reaction on MgO takes place on strong base sites such as the coordinatively unsaturated oxygen anions. Single oxides with higher electronegativity than MgO are less efficient to promote the reaction.

Acknowledgements

Authors thank Universidad Nacional del Litoral (UNL), Consejo Nacional de Investigaciones Científicas y Técnicas (CONICET) and Agencia Nacional de Promoción Científica y Tecnológica (ANPCyT) of Argentina, for the financial support of this work.

References

[1] A. Corma, S. Iborra, A. Velty, Chemical routes for the transformation of biomass into chemicals, Chem. Rev. 107 (2007) 2411–2502.
[2] J.W. Shabaker, G.W. Huber, J.A. Dumesic, Aqueous-phase reforming of oxygenated hydrocarbons over Sn-modified Ni catalysts, J. Catal. 222 (2004) 180–191.
[3] A. Corma, G.W. Huber, L. Sauvanaud, P. O'Connor, Processing biomass-derived oxygenates in the oil refinery: catalytic cracking (FCC) reaction pathways and role of catalyst, J. Catal. 247 (2007) 307–327.
[4] R.S. Karinen, A.O.I. Krause, New biocomponents from glycerol, Appl. Catal. A: Gen. 306 (2006) 128–133.
[5] Y. Zheng, X. Chen, Y. Shen, Commodity chemicals derived from glycerol, an important biorefinery feedstock, Chem. Rev. 108 (2008) 5253–5277.
[6] A. Corma, S.B.A. Hamid, S. Iborra, A. Velty, Lewis and Brønsted basic active sites on solid catalysts and their role in the synthesis of monoglycerides, J. Catal. 234 (2005) 340–347.
[7] N.O.V. Sonntag, Glycerolysis of fats and methyl esters. Status, review, and critique, J. Amer. Oil Chem. Soc. 59 (10) (1982) 795A–802A.
[8] J.I. Di Cosimo, V.K. Díez, C.R. Apesteguía, Base catalysis for the synthesis of α,β-unsaturated ketones from the vapor-phase aldol condensation of acetone, Appl. Catal. A: Gen. 13 (1996) 149–166.
[9] United States Pharmacopeia 32-NF27, 2008, 908.
[10] W.H. Tallent, R. Kleiman, Bis (trimethylsilyl) acetamide in the silylation of lipolysis products for gas-liquid chromatography, J. Lipid Res. 9 (1968) 146–148.
[11] D.S. Negi, F. Sobotka, T. Kimmel, G. Wozny, R. Schomaecker, Glycerolysis of fatty acid methyl esters. 1. Investigations in a batch reactor, J. Amer. Oil Chem. Soc. 8 (2007) 83–90.
[12] L. Jeromin, G. Wozny, P. Li, US Patent 6,127,561 (2000).
[13] T.F. Dossin, M.F. Reyniers, R.J. Berger, G.B. Marin, Simulation of heterogeneously MgO-catalyzed transesterification for fine-chemical and biodiesel industrial production, App. Catal. B: Environ. 67 (2006) 136–148.
[14] T. Kimmel, Kinetic investigation of the base-catalyzed glycerolysis of fatty acid methyl esters. PhD Thesis, Institut fur Chemie, TU, Berlin, Germany, 2004.
[15] A.E. Andreatta, L.M. Casás, P. Hegel, S.B. Bottini, E.A. Brignole, Phase equilibria in ternary mixtures of methyl oleate, glycerol, and methanol, Ind. Eng. Chem. Res. 47 (2008) 5157–5164.
[16] J. Barrault, Y. Pouillox, J. Clacens, C. Vanhove, S. Bancquart, Catalysis and fine chemistry, Cat. Today 75 (2002) 177–181.
[17] A. Corma, G.W. Huber, L. Sauvanaud, P. OïConnor, Biomass to chemicals: catalytic conversion of glycerol/water mixtures into acrolein, reaction network, J. Catal. 257 (2008) 163–171.
[18] R.T. Sanderson, Chemical Bonds and Bond Energy, 2nd ed., Academic Press, New York, 1976.
[19] J.I. Di Cosimo, V.K. Díez, M. Xu, E. Iglesia, C.R. Apesteguía, Structure and surface and catalytic properties of Mg–Al basic oxides, J. Catal. 178 (1998) 499–510.
[20] R. Philipp, K. Fujimoto, FTIR spectroscopic study of carbon dioxide adsorption/desorption on magnesia/calcium oxide catalysts, J. Phys. Chem. 96 (1992) 9035–9038.
[21] C. Morterra, G. Ghiotti, F. Boccuzzi, S. Coluccia, An infrared spectroscopic investigation of the surface properties of magnesium aluminate spinel, J. Catal. 51 (1978) 299–313.